ARTICLE

Density Functional Study of Physical and Chemical Properties of Nano Size Boron Clusters: B_n (n=13–20)

Murat Atiş[a], Cem Özdoğan[b*], Ziya B. Güvenç[c]

a. Department of Physics, University of Nevşehir, 50300 Nevşehir, Turkey
b. Department of Computer Engineering, Çankaya University, Balgat 06530 Ankara, Turkey
c. Department of Electronic and Communication Engineering, Çankaya University, Balgat 06530 Ankara, Turkey

(Dated: Received on March 27, 2009; Accepted on June 3, 2009)

Boron is an element that has ability to build strong and highly directional bonds with boron itself. As a result, boron atoms form diverse structural motifs, ultimately can yield distinct nano structures, such as planar, quasi-planar, convex, cage, open-cage, tubular, spherical, ring, dome-like, shell, capsule, and so on, *i.e.*, it can take almost any shape. Therefore, a deep understanding of the physical and chemical properties becomes important in boron cluster chemistry. Electronic and geometric structures, total and binding energies, harmonic frequencies, point symmetries, charge distributions, dipole moments, chemical bondings and the highest occupied molecular orbital−lowest unoccupied molecular orbital energy gaps of neutral B_n (n=13−20) clusters have been investigated by density functional theory (DFT), B3LYP with 6-311++G(d,p) basis set. Furthermore, the first and the second energy differences are used to obtain the most stable sizes. We have observed that almost all physical properties are size dependent, and double-ring tubular form of B_{20} has the highest binding energy per atom. The icosahedral structure with an inside atom is found as impossible as a stable structure for the size thirteen. This structure transforms to an open-cage form. The structural transition from two-dimensional to three-dimensional is found at the size of 20 and consistent with the literature. The calculated charges by the Mulliken analysis show that there is a symmetry pattern with respect to the x-z and y-z planes for the charge distributions. The unusual planar stability of the boron clusters may be explained by the delocalized π and σ bonding characteristic together with the existence of the multicentered bonding. The results have been compared to available studies in the literature.

Key words: Cluster, Boron, Density functional theory

I. INTRODUCTION

Boron due to its remarkable properties toward chemical bonding, *i.e.*, its ability to build strong and highly directional bonds with electron-donor atoms and itself, can form diverse clusters motifs, ultimately can yield distinct nano structures: planar, quasi-planar, convex, open-cage/cage, tubular, spherical, ring, etc. The confirmation that small all-boron clusters form planar/quasi-planar shapes rather than closed, nearly spherical clusters the way boranes do suggest that there are many more boron cluster shapes possible lying between the end points of the borane deltahedra and these planar boron clusters. Therefore, understanding of the physical and chemical properties becomes important in boron cluster chemistry. Ability of forming diverse structural motifs has attracted a lot of interest within the last several decades [1−8]. Further, this interest has also grown due to the possible technological applications such as high-energy density fuels [9], stable chemical insulators [10], hydrogen storage systems based on boron and its compounds [11].

Readers can find detailed literature review and discussions for the smaller sizes of boron clusters (n=2–12) in Ref.[12]. Therefore, here we will compare our results to directly related boron cluster studies within the range of n=13−20. There are a few studies in this range. For example, Boustani reported a systematic study on the neutral boron clusters, B_n (n=2−14) [13]. This study was carried out by applying *ab initio* quantum-chemical and Hartree-Fock self-consistent field (HF-SCF) methods (with 3-21G basis set) by using GAMESS-UK and Gaussian-92 programs. Fowler and Ugalde investigated structures and molecular orbitals of neutral, cationic and anionic B_{13} clusters using the density functional theory (DFT) (B3LYP/D95 and with 6-311G basis sets) with Gaussian-94 [14]. Cao and co-workers investi-

*Author to whom correspondence should be addressed. E-mail: ozdogan@cankaya.edu.tr

gated the structures of B_7, B_{10} and B_{13} boron clusters using full-potential linear-muffin-tin-orbital molecular-dynamics method [15]. Gu *et al.* studied structure and energetics of cationic B_{13} cluster using B3LYP/6-31G* with Gaussian-94 [16]. Aihara following the previous works [13,14,16] reported a correlation between aromaticity and topological resonance energy for B_{13} cluster [17]. Kawai and Weare calculated the electronic and geometric isomers of B_{13} clusters by using local density approximation [18]. They used simulating annealing to identify the lowest energy atomic configuration. There are very few systematic studies to investigate the boron clusters. A joint photoelectron spectroscopy (PES) with theoretical study for the size range of n=2–15 is reported recently [19]. A recent study is reported for the comprehensive analysis of chemical bonding in boron clusters [20] based on the previously determined geometries in Ref.[19]. Their reported energetically favored isomers have quasi-planar structures for the sizes of thirteen, fourteen, and fifteen with the following symmetry and electronic states C_s,$^2A'$, C_{2v},$^1A_1$, and C_1,^2A, respectively. Another combined PES and theoretical study was recently reported by Wang and co-workers on the structural stability and chemical bonding analysis of neutral, anionic, and dianionic states of B_{16} cluster [21]. In their study, it is reported that both B_{16} and B_{16}^- exhibits quasi-planar geometry whereas the addition of an electron leads to a perfectly planar B_{16}^{-2}. It is also reported that this dianionc cluster possesses a similar π bonding pattern of naphthalene and can be considered as an "all-boron naphthalene".

It is confirmed by both theoretical predictions and experimental observations that the most stable boron clusters are small and have planar/quasi-planar structures. The question of up to which size these 2D planar/quasi-planar structures remain as the most stable ones is the matter of interest. Several studies are reported for exploring the phase/structural transition from two-dimensional (2D) to three-dimension (3D). Kiran *et al.* investigated structure and photoelectron spectra of the neutral and anionic B_{20} clusters both experimentally and theoretically [22] using the Beckes three-parameter hybrid exchange functional [23] and the Lee-Yang-Parr non-local correlation functional [24] (B3LYP), 6-311+G*. It is proposed that B_{20} was the embryo of single-walled boron nanotubes for a planar-to-tubular structural transition in boron clusters. Marques and Botti calculated the optical response of the lowest-energy isomers of B_{20} family by using time-dependent DFT within a real-space, real-time scheme to reveal the question of the transition size [25]. They have shown that the optical spectroscopy can be applied to distinguish without ambiguity between the different low-energy members of the B_{20} family. The most stable neutral B_{20} isomer is clearly identified as tubular due to the presence of a very sharp resonance at about 4.8 eV. Highly accurate *ab initio* molecular-orbital methods (MP4(SDQ) and CCSD(T) calculations) have been employed to determine the relative stability among four low-lying neutral and anionic B_{20} isomers, particularly the double-ring tubular isomer versus three low-lying planar isomers by Zeng and co-workers [26]. Both calculations show that the double-ring is the lowest-energy structure and has a large negative nucleus-independent chemical shifts (NICS) and therefore strongly aromatic. Oger *et al.* claimed that boron cluster cations have been found to undergo a transition between quasi-planar and cylindrical molecular structures at B_{16}^+ [27]. For the cationic states of B_{17} and larger sizes, the cylindrical geometries dominate the low-energy structures and for neutral clusters, the structural transition occurs at B_{20}.

Our reported energetically favored isomers have a quasi-planar structure for the size of thirteen and convex structures for the sizes of fourteen and fifteen. Motivation behind our work is to understand size dependence of the physical and chemical properties of nano size bare neutral boron clusters by also focusing on a size range that has not been studied extensively before (with n=16–19). This work will fill a gap in the literature on the bare neutral boron clusters studies. We have studied different geometrical structures mainly grouped as planar/quasi-planar, convex, cage/open-cage, and tubular forms. As it is mentioned above, the basis set used in this study to stabilize the wave-functions and optimize the boron clusters, and to calculate all the physical quantities is the largest one to our knowledge for the size range of n=13–20. The number of the isomers are limited for the each group of geometrical structures since it is not possible to address for the many possible isomers with the used method and the basis set. The present set of isomers are carefully chosen based on the literature, such as the well known unusual planar stability of the boron clusters. Comparison of our findings with the available literature will contribute to the knowledge, and answers the question of sensitivity of the physical and chemical properties of the clusters to the size of the basis sets used. Furthermore, variation of the physical and chemical properties along the possible simple growth paths in the studied isomers can be analyzed. These obtained reliable structures will form good starting points for our further studies on boron compounds. The basis set used in this study, 6-311++G(d,p) is actually equivalent to 6-311+G(d) as the second + and p refer to hydrogen atoms. The reason that we consider using the 6-311++G(d,p) notation is our planned future work for investigating the hydrogenated boron clusters based on the presented study.

II. COMPUTATIONAL PROCEDURE

We have reached the final values by using three-stage procedure in the DFT framework (B3LYP). As the first step relatively small 6-31G basis set was employed, with tight SCF convergence criteria, for the lo-

DOI:10.1088/1674-0068/22/04/380-388

cal minima search on the potential-energy surface of the cluster to obtain reliable initial guess of the geometry. Secondly, starting from this equilibrium structure, the wave function was stabilized [24,28] by using the larger 6-311++G(d,p) basis set. As the last step, full geometry optimization and vibrational frequency calculations were performed at the same level. Quadratically convergent SCF procedure was used for the optimization (if converges, otherwise tight SCF convergence criteria was considered) at the B3LYP/6-311++G(d,p) level of theory. We have reported only the final values in the present work. All computations of the boron clusters were carried out using the Gaussian-03 [29] installed on our parallel computation laboratory. This size range n is computationally highly demanding with the B3LYP/6-311++G(d,p) basis set, therefore, parallel computation had to be utilized (Linda package is used to fulfill this requirement). We have studied in detail some of the interesting geometric structures, such as planar, quasi-planar, ring, tubular, convex, cage, open-cage, and capsule, of the neutral B_n (n=13–20) clusters by considering the electronic structures, total and binding energies, the first and the second energy differences between the consecutive cluster sizes, harmonic frequencies, point symmetries and HOMO-LUMO energy gaps, and average of the bond distances of the neutral boron clusters. In this study, it is aimed to investigate the effect of increasing the system sizes on the physical properties of the clusters instead of exploring the lowest energy isomers of the B_n (n=13–20) clusters. Beside, it may be not reasonable to search the global minima on the potential energy surface for the lowest energy isomers with B3LYP/6-311++G(d,p) level of theory. It is observed in our previous study [12] for the B_n (n=2–12) clusters that the lowest energy isomers have generally the lowest spin multiplicities, especially for the larger sizes. Despite of this observation, we have also performed optimization calculations for the lowest energy isomers with higher spin multiplicities to improve the reliability of our predicted geometries. The optimized geometry coordinates for a given size (between 13 and 20) were used as an input for these further calculations with higher spin multiplicities, namely triplet, quintet, and quartet, sextet for even and odd number of electrons; respectively. The obtained energies with high spin multiplicities are all lower compared to the lowest spin multiplicity. Therefore, we report and discuss only the lowest spin multiplicities (singlet and doublet) for the lowest energy isomers of the clusters. The binding energies of the isomers per atom are calculated by using the following expression:

$$E_{\rm b} = \frac{E_n - nE_1}{n} \tag{1}$$

here, $E_{\rm b}$ is the binding energy (BE) per atom, E_1 and E_n are the energy of a single neutral boron atom, and that of the n-atom neutral boron cluster, respectively. The first and the second energy differences, ΔE_1 and ΔE_2 are calculated from the relations:

$$\Delta E_1 = E_n - E_{n-1} \tag{2}$$

$$\Delta E_2 = E_{n+1} + E_{n-1} - 2E_n \tag{3}$$

where the values of subscripts show the sizes of the clusters, and the energies are the corresponding total BEs of those sizes. These differences are used to test the relative stabilities of the clusters. Furthermore, the growth mechanisms of different configurations and possible simple growth-path (growth with a minor structural change) are also investigated. In addition changes in the chemical and physical properties ($E_{\rm b}$, HOMO-LUMO energy gap, range of vibrational frequencies and average bond length) are studied in each group (planar, quasi-planar, cage, etc.) as a function of the size.

III. RESULTS AND DISCUSSION

A. Structural stability

We have obtained some of the stable isomers of B_n (n=13–20) clusters, which are shown in Figs. 1 and 2. Here, the lowest energy isomer means the first isomer (denoted by 1) of that size and the second lowest is the second isomer (denoted by 2) and so on. The point groups, electronic states, total and the binding energies of the isomers, the lowest and the highest frequencies, HOMO-LUMO energy gaps (for α- and β-electrons), and the average of the bond distances of the clusters are given in Table I. Only the singlet or doublet spin multiplicities are considered for all the isomers depending on the even or odd number of boron atoms (with the exception B_{14}-4). Zero point energy corrections (ZPE) are included in the isomer energies. The binding energies, and the first and the second energy differences of the lowest energy structures are illustrated in Figs. 3 and 4, respectively. The binding energies per atom for all the isomers are listed in Table I and they are also presented in Fig.3 for all the groups of the geometrical structures. So that there are one or more points for the same size referring to the different isomers of the same size. This helps us to understand the variation of the binding energies with the size within each of the groups of physical structures. In general the BE per atom is gradually increasing with the size for the double rings, capsules, and quasi-planar forms, however, some significant and small oscillations are also observed. It is reasonable and acceptable for that non-smooth behavior since the reported size is very little compared to the bulk limit (the BE per atom for boron is about −6 eV/atom in the bulk limit), so that there are very large surfaces and number of dangling bonds. For example, the cage forms in Fig.3 have a significant peak created by the body atom (inside the shell) of n=13, *i.e.*, for this size the averaged bond distances value was the highest value at the studied size range. This increase in the bond length also points to a decrease in

DOI:10.1088/1674-0068/22/04/380-388

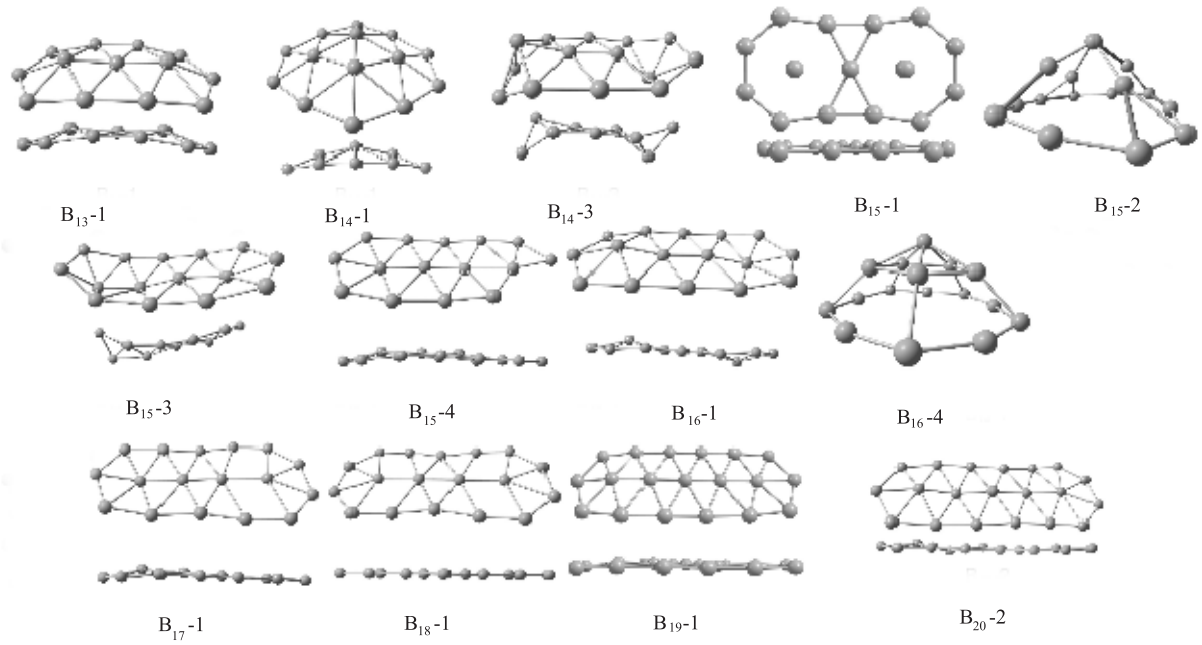

FIG. 1 Planar, quasi-planar, and convex isomers of B_n (n=13–20) clusters.

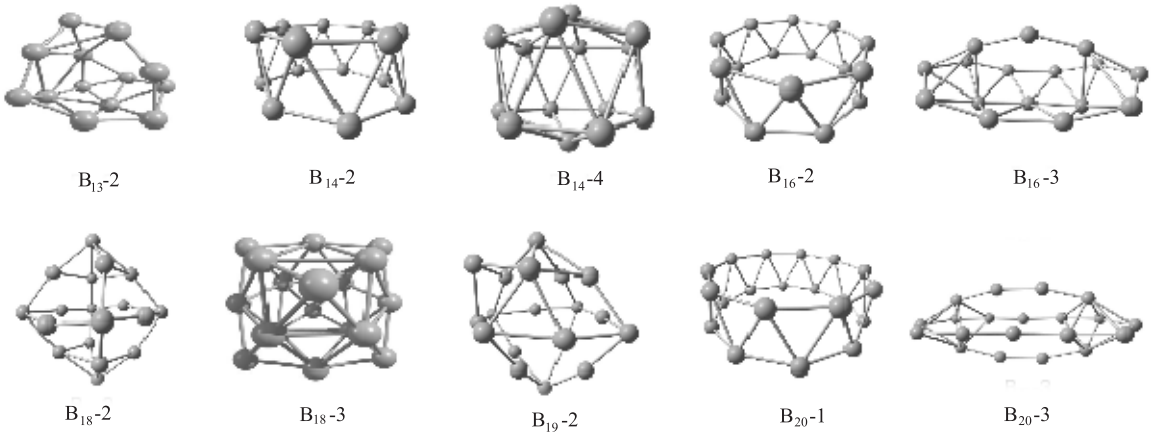

FIG. 2 Cage, open-cage, tubular, and capsule structures of B_n (n=13−20) clusters.

the strength of the bonds and consequently decrease in the binding energy. On the other hand, it is suggested by Hanley *et al.* that B_{13}^+ should have an icosahedral structure with one encapsulated boron atom in the cluster center rather than capping a triangular face [7]. Together with their conclusion and our resulting icosahedral B_{13} cluster with five imaginary frequencies, we further investigated this structure to find out the stationary point in the potential energy surface by jiggling the structure and then re-optimizing since jiggling is one of the suggested procedures to remove imaginary frequencies. The obtained final structure with a stationary point is no more icosahedral structure but rather amorphous. Our conclusion is that the icosahedral structure for boron clusters is not possible. The explanation for this significant peak is also given while we are discussing the charge distributions and dipole moments. The other cages and structures for all the sizes have only the surface atoms. In the case of the quasi-planar structures, there is also a peak which belongs to the third isomer of the B_{14}. This isomer has four atoms which are out of plane; two of them are above and the other two are below the plane. On the other hand, the smaller oscillations in the BE may be caused by the missed global minimum structures for those sizes. However, the oscillations in the binding energies for the small size of the clusters are also observed in the literature for many different elements. The lowest BE per atom obtained in this work is −4.78 eV/atom for the double-ring structure of the B_{20}. From the binding energies, one can conclude that the quasi-planar and double-ring geometric structures are more favored by the boron atoms. The

DOI:10.1088/1674-0068/22/04/380-388

TABLE I Structural geometries, point groups (PG), electronic states (ES), average bond lengths (d), total energies (TE) and binding energies (BE), averaged BE, BE per atom, frequency ranges, and HOMO-LUMO energy gaps (for α- and β-electrons) of the isomers of B_n (n=13–20) clusters.

n	isomer	Geom. group	PG	ES	d/Å	TE/eV	BE/eV	BE/eV		Frequency/cm^{-1}		HOMO-LUMO gap	
								Aver.	Per atom	Lowest	Highest	$\alpha-e^-$	$\beta-e^-$
13	1	Quasi planar	C_{2v}	^{2}A	1.67	−8783.69	−59.32	−58.19	−4.56	82	1302	1.83	2.44
13	2	Cage	C_s	^{2}A	1.75	−8781.43	−57.06		−4.39	158	1304	2.34	1.76
14	1	Convex	C_{2v}	^{1}A	1.68	−9459.95	−64.48	−62.14	−4.51	140	1324	2.34	
14	2	Double ring	C_2	^{1}A	1.67	−9458.37	−62.90		−4.49	73	1249	1.41	
14	3	Quasi planar	C_s	^{1}A	1.70	−9456.60	−61.13		−4.37	57	1380	1.57	
14	4	Cage	C_2	^{3}A	1.67	−9455.51	−60.03		−4.29	46	1100	2.85	1.58
15	1	Planar	C_s	^{2}A	1.58	−10135.94	−69.36	68.59	−4.62	80	1544	2.48	2.29
15	2	Convex	C_2	^{2}A	1.67	−10135.16	−68.58		−4.57	131	1473	2.50	2.20
15	3	Quasi planar	C_s	^{2}A	1.68	−10134.86	−68.28		−4.55	82	1345	2.07	2.09
15	4	Quasi planar	C_s	^{2}A	1.68	−10134.72	−68.14		−4.54	57	1415	2.41	2.40
16	1	Quasi planar	C_s	^{1}A	1.68	−10812.15	−74.47	−73.42	−4.65	67	1335	2.14	
16	2	Double ring	D_2		1.64	−10811.53	−73.85		−4.62	152	1272	1.67	
16	3	Capsule	C_{2v}	^{1}A	1.73	−10810.64	−72.96		−4.56	137	1330	3.13	
16	4	Convex	C_{5v}	^{1}A	1.72	−10810.08	−72.39		−4.53	77$^{(2)a}$	1375	1.67	
17	1	Quasi planar	C_s	^{2}A	1.68	−11487.98	−79.19	−79.19	−4.66	69	1543	1.65	1.81
18	1	Quasi planar	D_{2h}	^{1}A	1.68	−12164.10	−84.21	−82.93	−4.68	57	1562	1.51	
18	2	Cage	S_2	^{1}A	1.69	−12162.18	−82.29		−4.57	335	1193	2.13	
18	3	Capsule	C_s	^{1}A	1.69	−12162.18	−82.28		−4.57	334	1193	2.13	
19	1	Quasi planar	C_s	^{2}A	1.68	−12840.37	−89.36	−87.27	−4.70	31	1327	2.55	1.33
19	2	Cage	C_s	^{2}A	1.73	−12836.17	−85.17		−4.48	208	1162	2.04	1.85
20	1	Double ring	D_{2d}		1.66	−13517.68	−95.57	−94.30	−4.78	113	1286	2.48	
20	2	Quasi planar	C_s	^{1}A	1.69	−13516.79	−94.69		−4.73	45	1540	2.18	
20	3	Capsule	D_{2h}	^{1}A	1.73	−13514.75	−92.65		−4.63	135	1432	2.11	

[a] Number of imaginary frequencies is given in parenthesis in the lowest frequency column.

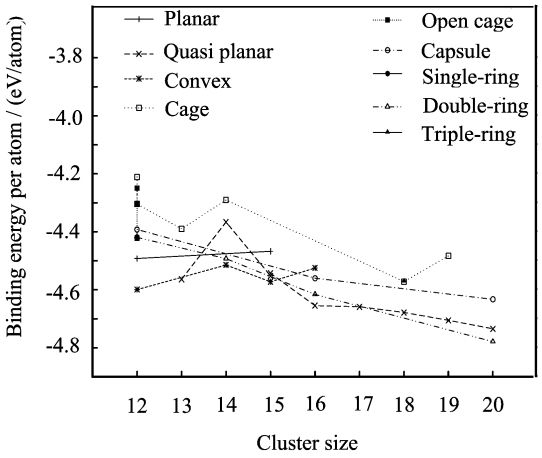

FIG. 3 Binding energies per atom for B_n (n=12−20) clusters. Values for the n=12 are taken from Ref.[12].

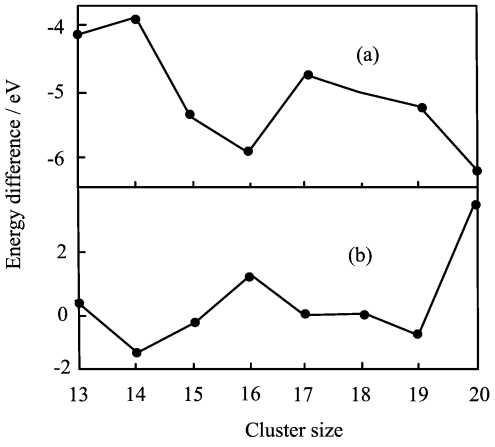

FIG. 4 First (a) and (b) second energy differences of B_n (n=13–20) clusters.

relative stability of the clusters can be extracted from the first and the second energy differences, and they are presented in Fig.4 (only the binding energies of the first isomers are considered). As seen from the figures the B_{16}-1 (quasi-planar) and B_{20}-1 (double-ring) structures are relatively more stable. On the other hand, the B_{14}-1 (convex), B_{17}-1 (quasi-planar), and the B_{19}-1

DOI:10.1088/1674-0068/22/04/380-388

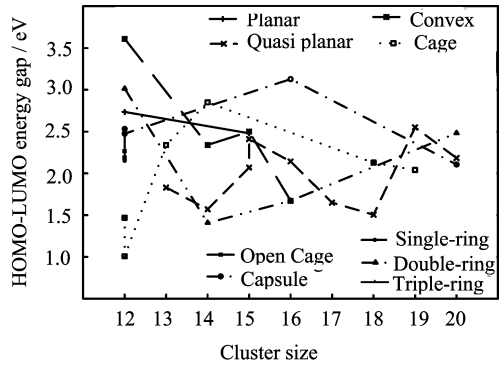

FIG. 5 HOMO-LUMO energy gaps for B_n (n=12–20) clusters. Values for the n=12 are taken from Ref.[12]

(quasi-planar) are relatively less stable clusters.

As known, generally the larger value of the HOMO-LUMO energy gap refers to a higher value of the chemical hardness [30]. Therefore it is important to explore different stable isomers and sizes to understand their relative chemical hardness and reactive features, and the variation of the energy gaps with the size and the type of the geometric structures. The HOMO-LUMO energy gaps for the α- and β-electrons are given in Table I. In Fig.5, only the energy gaps of the α-electrons for all the isomers are presented. There is somewhat correlation between the binding energies (stability) and the energy gaps of the structures. Energetically more favored structures are chemically harder, and less favored structures have smaller energy gaps. As seen, the HOMO-LUMO energy gap is increasing as the diameter of the double-ring increases from n=14 to n=20. The binding energy per atom is also increasing from n=14 to n=20. From the trends of the double-ring forms (Figs. 3 and 4), the BE and the HOMO-LUMO energy gap for n=18 are higher compared to those of the triple-ring structure. This correlation between the BE and the energy gap is also seen clearly for the quasi-planar structures; the most of the quasi-planar structures have higher binding energies and over 2.0 eV of the energy gaps. The least correlations are observed for the cage, capsule, and convex forms.

In general, the vibrational frequency ranges of the structures are increasing with the size of the tubular, planar/quasi-planar, convex, and capsule forms (see Fig.6). The number of imaginary frequencies obtained after optimization is also reported in Table I (only for B_{16}-4 in the present study). The vibrational frequencies were used for the characterization of stationary points and the ZPE corrections. All the stationary points were positively identified for the minima (no imaginary frequency) or transition states (only one imaginary frequency) or higher-order saddle points (more than one imaginary frequency). The smallest frequency ranges are observed for the double-ring structure of the B_{12} and for the cage form of the B_{18}-2. The largest frequency ranges are observed for the planar (B_{15}-3), single- and

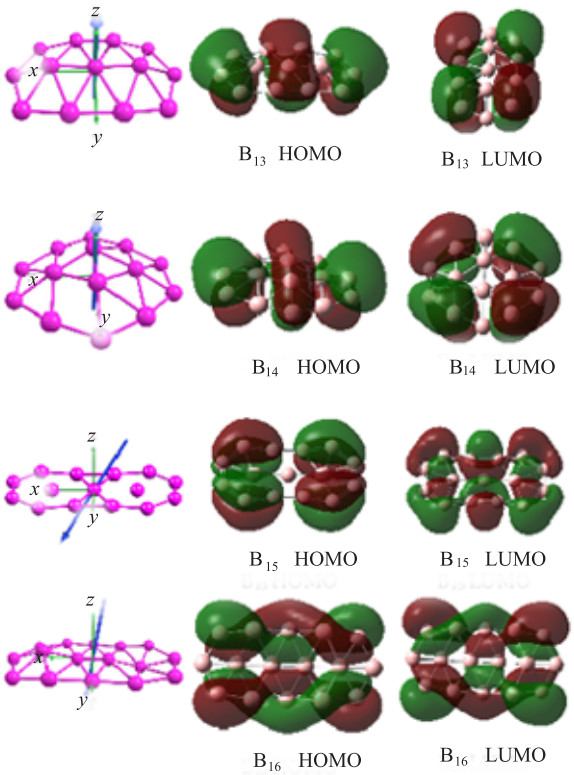

FIG. 6 Dipole moments, HOMO-LUMO molecular orbital pictures for B_n (n=13–16) clusters.

triple-ring forms (B_{12}-11 and B_{18}-3, respectively).

The average bond lengths are tabulated in Table I. For some of the geometric forms; the double-ring, quasi-planar, and the capsule, the average values more or less remain constant as the size and the BE per atom increase. On the other hand, the cage forms of the B_{13} (because of the body-atom in the shell structure) have the largest average bond lengths since the body-atom pushes the shell atoms outward. This structure is energetically the least favored in the size range of n=12–20 and eventually resulted as an open-cage structure by further investigation.

One may define a possible "simple" growing path within the range of the studied isomers of the n=12–20 boron clusters. This simple growth-path is observed along the B_{14}-1→B_{15}-4→ B_{16}-4 (among the convex forms), and the B_{15}-2 or B_{15}-3→B_{16}-1→B_{17}-1→ B_{18}-1→B_{19}-1→B_{20}-2 (among the quasi-planar forms). These convex and quasi planar forms, generally speaking, have the highest BE per atom values for the studied size range and isomers (see Fig.3). In the former path, a boron atom is added first on the top of the structure to obtain fifteen-atom cluster and then another boron atom is inserted into the 4-atom ring for producing sixteen-atom one. In the latter path, the quasi-planar structures are formed by inter linked nearly flat hexagonal and pentagonal pyramids. In order to form a hexagonal ring at one of the ends of the B_{15}-2 or B_{15}-3,

DOI:10.1088/1674-0068/22/04/380-388

one needs to add one more boron atom into the ring. Adding one more boron atom to one of the ends of the B_{16}-1 creates a heptagonal structure at that end (forms the B_{17}-1). Similarly adding one more boron to the B_{17}-1 creates another heptagonal structure at the other end (forms the B_{18}-1). In order to form B_{19}-1 from B_{16}-1 one has to add three more boron atoms to one of the ends of the B_{16}-1.

B. Charge distributions and dipole moments

Charge distributions of the isomers have also been investigated in this work. The largest differences on the calculated charge values for the atoms of the clusters studied in the size range are observed at the central atom of the B_{13}-2 icosahedral form. The anomalous stability of the B_{13}^+cluster is reported in the works of Hanley *et al.* [7] and several theoretical studies. Hanley *et al.* suggested that B_{13}^+ should have an icosahedral structure with one encapsulated boron atom in the cluster center rather than capping a triangular face on the basis of its anomalously high experimental stability. But, the theoretical studies suggest that the most stable structure for the B_{13}^+ is a planar. This situation is also proved in our studies for both neutral and cationic states (in preparation for submission). The calculated charge for the central atom is 8.122 while the Mulliken charges for the surrounding atoms vary between −0.569 and −0.799. The charge distribution among the atoms could be said as non-uniform for this isomer. This unrealistic situation is not seen for the resulting stable open-cage structure (see Fig.3). On the other hand, the isomers found at the possible simple growth path exhibit an almost symmetric charge distribution pattern. The calculated charges by the Mulliken analysis (not given as figure) show that there is a symmetry pattern with respect to the x-z and y-z planes for the charge distributions. This finding is also supported with the direction of the dipole moment and also with the electron occupancies in Figs. 6 and 7 (discussed only for the HOMO pictures). In these figures, these properties are given only for the most stable isomers (denoted by 1). Calculated dipole moments with field-independent basis for the clusters of B_{13}-1 and B_{14}-1 have only non-zero component in the z-direction and the charge distributions are almost perfectly symmetric with respect to the x-z and y-z planes. Besides, the molecular orbital patterns are similar and have delocalized π bonding nature. On the other hand, the dipole moments have some components other than z-direction for the B_{16}-1 and B_{17}-1 clusters. The charge distribution for these clusters are nearly perfect in symmetry consideration and in terms of molecular orbital pictures (the presence of the delocalized σ bonding together with π characteristic). This distortion in the symmetric charge distribution is also observed for the B_{15}-1 and B_{19}-1 clusters. However, the effect of this distortion on the HOMO pictures is not observed as the considerable amount occupation of the σ bonding. There are two sizes that dipole moment has no magnitude, namely B_{18}-1 and B_{20}-1 clusters. The B_{18}-1 cluster has a perfectly symmetric charge distributions with respect to the x-z and y-z planes. The distribution pattern of the charges among the atoms is particularly determined for the tubular structures. The calculated charges by the Mulliken analysis are alike and also small/very small for all the atoms in these tubular structures. The charge distribution for the B_{14}-2 and B_{20}-1 tubular structures show a mixing of positively and negatively charged atoms at each of the layers and have zero net charge for each of the layers. On the other hand, one layer of the B_{16}-2 isomer (double ring) has the atoms with very small positive charges and the other layer with a combination of the positive and negative charges. The triple ring B_{18}-3 isomer exhibits a different charge distribution pattern. The middle layer contains (for all the atoms) negative charges. The charges are close in value for the atoms in each layer but the charges of the middle layer of atoms are twice of those of upper and lower layer atoms. The structures with some interior atoms mostly have larger positive charges positioned at the center of the cluster and surrounded by the negatively charged atoms.

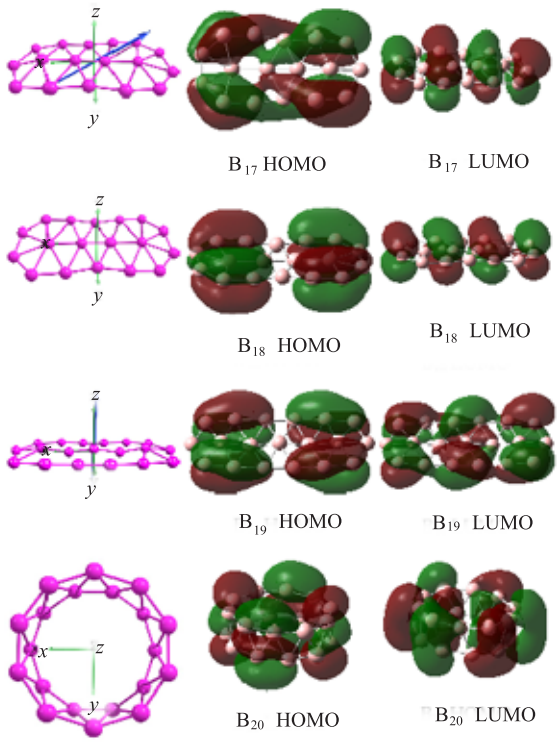

FIG. 7 Dipole moments, HOMO-LUMO molecular orbital pictures for B_n (n=17–20) clusters.

C. Chemical bonding

The HOMO and LUMO pictures of molecular orbitals for α-electrons are depicted in Figs. 6 and 7 for the

DOI:10.1088/1674-0068/22/04/380-388

neutral B_{13-20} clusters. In this study, only the HOMO pictures will be discussed to reveal the reasons that govern the stability of the boron clusters. The optimized geometries of B_{13}-1 cluster is convex structure. The HOMO picture of the size thirteen cluster shows delocalized π bonding characteristic. The Wiberg bond index (WBI) analysis suggests the existence of the multicentered bonding. It is found that the accepted Lewis structure has twenty two 2-center (BD) bonds and zero lone pair (LP) bonds by natural bond orbital (NBO) analysis. The molecular orbitals of B_{13}-1 and B_{14}-1 are similarly formed by the highly delocalized, multicentered π bondings. The obtained BD and LP bonds for the B_{14}-1 are (10,11) and (22,1), respectively. The WBI analysis predicts the existence of the multicentered bonds for the B_{15}-1. The B_{16}-1 and B_{17}-1 clusters have strongly delocalized π and σ bonding. The WBI analysis suggests the existence of the multicentered bonds together with the three-centered bonds for both sizes. The numbers of BD and LP bonds are found as (15,9) and (20,6) for the B_{16}-1 and B_{17}-1 clusters, respectively, according to the NBO analysis. Also, B_{18}-1 and B_{19}-1 clusters exhibit a highly delocalized π bonding nature according to the HOMO pictures and the WBI analysis. In terms of the NBO analysis, the numbers of BD and LP bonds are given as (16,11) and (23,6) for the B_{18}-1 and B_{19}-1 clusters, respectively. The HOMO picture of B_{20}-1 cluster is formed by strongly delocalized π and σ bonding. The HOMO and HOMO-1, HOMO-2 and HOMO-3, HOMO-4 and HOMO-5 orbitals of the B_{20}-1 are found to be doubly degenerate. The number of three-center bonds for the B_{20}-1 neutral is found to be ten by the WBI analysis and that of the obtained BD bonds by the NBO analysis is twenty and that of the LP bonds is ten. We observed that the size 20 is the critical size of the structural transition from 2D to 3D [22,26]. The highest binding energy per atom value in the studied size range together with small averaged distance (see Table I) contribute to the stability of the double-ring isomer (becoming the lowest energy configuration) of the B_{20}-1.

IV. CONCLUSION

The first finding to be reported for boron cluster is the instability of the icosahedral structure with a central atom. This structure is unable to sustain the stability and transforms to an open-cage structure as the central atom becoming a surface atom. In general, the lowest energy structures of the boron clusters observed in this work are the quasi-planar and the convex forms except the B_{20}-1 which is a double-ring. These findings are in agreement with the related works on the small boron clusters [12,13]. On the other hand, we have also obtained energetically higher planar/quasi-planar isomers, *e.g.*, B_{15}-2 and B_{15}-3. Another interesting structures are the tubular forms, *e.g.*, B_{12}-5, B_{14}-2, B_{16}-2, B_{18}-3, and B_{20}-1. In general the tubular forms have less binding energies compared to the quasi-planar forms. However, the B_{20}-1 double-ring structure has the highest BE per atom among all the isomers (see Fig.3). Kiran *et al.* recently reported that neutral and anionic tubular forms of B_{20} have higher binding energies per atom than those of the planar, quasi-planar and convex structures [22]. This result is in very good agreement with our findings. We have observed somewhat correlation between the binding energies of the isomers and the HOMO-LUMO energy gaps. The calculated charges by the Mulliken analysis (not given as figure) show that there is a symmetry pattern with respect to the x-z and y-z planes for the charge distributions. This charge distribution pattern is observed as almost perfectly symmetric for the B_{13}-1 and B_{14}-1 clusters, as nearly perfect symmetric for the B_{16}-1 and B_{17}-1 clusters, as perfectly symmetric for the B_{18}-1 cluster, and as distortion of the symmetry for the B_{15}-1 and B_{19}-1 clusters. The charge distribution for the B_{20}-1 tubular structure exhibits a different aspect such as the minimization of the charge distribution (being small/very small in value for all the atoms). Furthermore, the charge distribution for the B_{20}-1 tubular structure shows a mixing of positively and negatively charged atoms in each of the layers and have zero net charge for the each of the layers. The structures with some interior atoms mostly have larger positive charges positioned at the center of the cluster and surrounded with the negatively charged atoms. The longest possible simple growth-path is observed among the quasi-planar structures; the B_{15}-2 or B_{15}-3→B_{16}-1→B_{17}-1→B_{18}-1→B_{19}-1→B_{20}-2. Along this path the BE per atom is gradually increasing. The isomers found at the possible simple growth path exhibit an almost symmetric charge distribution pattern. The unusual planar stability of the boron clusters may be explained by the delocalized π and σ bonding characteristic together with the existence of the multicentered bonding. Although we do not have a precise explanation for the structural transition from 2D to 3D at the size of 20, the highest BE per atom value in the studied size range together with the small averaged distance, comparatively different charge distribution pattern and double degeneracy in the molecular orbitals may contribute to the stability of the double-ring isomer as being the energetically most favored isomer.

The existence of the unusual planarity of small boron clusters are confirmed both by theoretically and experimentally. Planar boron clusters are analogous to hydrocarbons in their π-bonding patterns and can be classified according to the Hückel rules for aromaticity and antiaromaticity for hydrocarbon molecules. The structural transformation from 2D to 3D depends on the charge state and predicted to occur at the sizes of sixteen and twenty for cationic and neutral states, respectively. Together with this charge state dependency for the structural transformation and relatively few studies on the size range of seventeen and nineteen, there

DOI:10.1088/1674-0068/22/04/380-388

should be more effort devoted to elucidate the physical and chemical properties of boron clusters for this range. The next simple question arises as: when will the bulk-like cage structures appear? Since it is known that all known bulk boron allotropes are based on different arrangements of B_{12} icosahedra.

V. ACKNOWLEDGMENTS

This work was supported by the Scientific and Technical Council of Turkey (TUBITAK) (No.105T084) and in part by Çankaya University. The computations were performed at Çankaya University and in part at the ULAKBİM High Performance Computing Center at the Turkish Scientific and Technical Research Council.

[1] H. Kato and K. Yamashita, Chem. Phys. Lett. **190**, 361 (1992).
[2] R. Kawai and J. H. Weare, J. Chem. Phys. **95**, 1151 (1991).
[3] P. J. Bruna and J. S. Wright, J. Chem. Phys. **91**, 1126 (1989).
[4] I. Carmichael, J. Chem. Phys. **91**, 1072 (1989).
[5] P. A. Serena, A. Baratoff, and J. M. Soler, Phys. Rev. B **48**, 2046 (1993).
[6] A. K. Ray, I. A. Howard, and K. M. Kanal, Phys. Rev. B **45**, 14247 (1992).
[7] L. Hanley, J. L. Whitten, and S. L. Anderson, J. Phys. Chem. **92**, 5803 (1988).
[8] M. D. Cox, D. J. Trevor, R. L. Whetten, E. A. Rohlfing, and A. Kaldor, J. Chem. Phys. **84**, 4651 (1986).
[9] D. MeiKohn, Combust Flame **353**, 733 (1985).
[10] M. S. Reisch, Chem. Eng. News **65**, 9 (1987).
[11] E. Fakiroğlu, Y. Yürüm, and T. N. Veziroğlu, Int. J. Hydrogen Energy **29**, 1371 (2004).
[12] M. Atiş, C. Özdoğan, and Z. B. Güvenç, Int. J. Quantum Chem. **107**, 729 (2007).
[13] I. Boustani, Phy. Rev. B **55**, 16426 (1997).
[14] J. E. Fowler and J. M. Ugalde, J. Phys. Chem. A **397**, 104 (2000).
[15] P. L. Cao, Z. Zhao, B. X. Li, B. Song, and X. Y. Zhou, J. Phys: Cond. Matter **13**, 5065 (2001).
[16] F. L. Gu, X. Yang, A. C. Tang, H. Jiao, and P. V. R. Schleyer, J. Comp. Chem. **19**, 203 (1998).
[17] J. Aihara, J. Phys. Chem. A **105**, 5486 (2001).
[18] R. Kawai and J. H. Weare, Chem. Phys. Lett. **191**, 311 (1992).
[19] A. N. Alexandrova, A. I. Boldyrev, H. J. Zhai, and L. S. Wang, Coor. Chem. Rev. **250**, 2811 (2006).
[20] D. Y. Zubarev and A. I. Boldyrev, J. Comput. Chem. **28**, 251 (2006).
[21] A. P. Sergeeva, D. Y. Zubarev, H. J. Zhai, A. I. Boldyrev, and L. S. Wang, J. Am. Chem. Soc. **130**, 7244 (2008).
[22] B. Kiran, S. Bulusu, H. J. Zhai, S. Yoo, X. C. Zeng, and L. S. Wang, Proc. Natl. Acad. Sci. USA **102**, 961 (2005).
[23] A. D. Becke, J. Chem. Phys. **98**, 5468 (1993).
[24] C. Lee, W. Yang, and R. G. Parr, Phys. Rev. B **37**, 785 (1988).
[25] M. A. L. Marques and S. Botti, J. Chem. Phys. **123**, 014310 (2005).
[26] W. An, S. Bulusu, Y. Gao, and X. C. Zeng, J. Chem. Phys. **124**, 154310 (2006).
[27] E. Oger, N. R. M. Crawford, R. Kelting, P. Weis, M. M. Kappes, and R. Ahlrichs, Angew. Chem. Int. Ed. **46**, 8503 (2007).
[28] R. Seeger and J. A. Pople, J. Chem. Phys. **66**, 3045 (1977).
[29] M. J. Frisch, G. W. Trucks, H. B Schlegel, G. E. Scuseria, M. A. Robb, J. R. Cheeseman, J. A. Montgomery, Jr., T. Vreven, K. N. Kudin, J. C. Burant, J. M. Millam, S. S. Iyengar, J. Tomasi, V. Barone, B. Mennucci, M. Cossi, G. Scalmani, N. Rega, G. A. Petersson, H. Nakatsuji, M. Hada, M. Ehara, K. Toyota, R. Fukuda, J. Hasegawa, M. Ishida, T. Nakajima, Y. Honda, O. Kitao, H. Nakai, M. Klene, X. Li, J. E. Knox, H. P. Hratchian, J. B. Cross, V. Bakken, C. Adamo, J. Jaramillo, R. Gomperts, R. E. Stratmann, O. Yazyev, A. J. Austin, R. Cammi, C. Pomelli, J. W. Ochterski, P. Y. Ayala, K. Morokuma, G. A. Voth, P. Salvador, J. J. Dannenberg, V. G. Zakrzewski, S. Dapprich, A. D. Daniels, M. C. Strain, O. Farkas, D. K. Malick, A. D. Rabuck, K. Raghavachari, J. B. Foresman, J. V. Ortiz, Q. Cui, A. G. Baboul, S. Clifford, J. Cioslowski, B. B. Stefanov, G. Liu, A. Liashenko, P. Piskorz, I. Komaromi, R. L. Martin, D. J. Fox, T. Keith, M. A. Al-Laham, C. Y. Peng, A. Nanayakkara, M. Challacombe, P. M. W. Gill, B. Johnson, W. Chen, M. W. Wong, C. Gonzalez, and J. A. Pople, *Gaussian 03, Revision C.02*, Wallingford CT: Gaussian, Inc., (2004).
[30] R. G. Pearson, *Chemical Hardness*, Weinheim: Wiley-VCH Verlag, (1997).

DOI:10.1088/1674-0068/22/04/380-388